

Effective pair potentials for spherical nanoparticles

Ramses van Zon

*Chemical Physics Theory Group, Department of Chemistry, University of Toronto,
80 Saint George Street, Toronto, Ontario, Canada M5S 3H6*

(Dated: 22 September 2008)

An effective description for spherical nanoparticles in a fluid of point particles is presented. The points inside the nanoparticles and the point particles are assumed to interact via spherically symmetric additive pair potentials, while the distribution of points inside the nanoparticles is taken to be spherically symmetric and smooth. The resulting effective pair interactions between a nanoparticle and a point particle, as well as between two nanoparticles, are then given by spherically symmetric potentials. If overlap between particles is allowed, the effective potential generally has non-analytic points, but for each effective potential the expressions for different overlapping cases can be written in terms of one analytic auxiliary potential. Effective potentials for hollow nanoparticles (appropriate e.g. for buckyballs) are also considered, and shown to be related to those for solid nanoparticles. Finally, explicit expressions are given for the effective potentials derived from basic pair potentials of power law and exponential form, as well as from the commonly used London-Van der Waals, Morse, Buckingham, and Lennard-Jones potential. The applicability of the latter is demonstrated by comparison with an atomic description of nanoparticles with an internal face centered cubic structure.

PACS numbers: 62.23.Eg, 36.40.-c, 02.30.Mv

I. INTRODUCTION

Nanoparticles,^{1,2,3} quantum dots,⁴ colloidal suspensions,^{5,6} and globular proteins⁷ are examples of physical systems in which small nanometer or micron-sized clusters of particles are suspended in a fluid. Such systems have applications ranging from material coatings to drug delivery.^{8,9} For colloidal systems, collective behavior has been the focus of much research,^{6,10} while nanoclusters are often studied as isolated objects,^{11,12,13,14,15} despite interesting collective phenomena such as the increased heat conductance in dilute nanoparticle suspensions² and self-assembly.⁶

To study the collective properties of nanoparticles in suspension, one would expect that a detailed description of the internal structure of the clusters is not necessary, especially if the nanoparticles are more or less solid. On the other hand, a description in terms of hard spheres would probably be too crude for nanoparticles since typical atomic interaction ranges are on the order of Ångströms. The aim of this paper is to give a general effective description of nanoparticles which retains a level of detail beyond the hard sphere model and which is intended to be used in the study of the collective behavior of nanoparticles, either numerically or analytically. The starting point of the description is to assume that each nanoparticle is composed of particles with fixed relative positions, interacting with the point particles in the fluid and their counterparts in other nanoparticles through spherically symmetric pair potentials. It is furthermore assumed that the nanoparticles may be modeled as spheres

with a smooth spherically symmetric density of constituents, which can be viewed as a smoothing procedure for the interactions. In particular, solid and hollow spheres of uniform density are considered in detail, since these are suitable for describing solid nanoclusters and buckyballs (or similar structures), respectively. The spherical smoothing procedure results in spherically symmetric effective interaction potentials for nanoparticles and point particles, and consequently leads to a description of a nanoparticle as a single particle instead of as a collection of particles.

Similar approaches to the problem of constructing effective potentials have been used before, but only for specific cases.^{1,13,14,15,16,17} The current paper is devoted to the general method of deriving effective pair potentials for nanoparticles from the basic pair potential of their constituents. The possibility of overlapping and embedded particles is specifically treated as well.

The paper is structured as follows. In Sec. II, the general smoothing procedure is explained. Properties of the resulting effective potentials are explored in Sec. III, with special consideration for the difference between non-overlapping and overlapping particles, which results in a reformulation of the non-analytic effective potentials in terms of analytic auxiliary potentials. In Sec. IV, the formalism is extended to include hollow nanoparticles. For uniform solid and hollow nanoparticle structures, explicit effective potentials for a nanoparticle and a point particle and for different nanoparticles are worked out in Sec. V for the London-van der Waals potential, the exponential potential, the Morse potential, the (modified) Buckingham potential, and the Lennard-Jones potential. Section VI addresses the applicability of the effective potentials by comparison with an atom-based nanoparticle model. A discussion in Sec. VII concludes the paper.

II. SMOOTHING PROCEDURE FOR NANOPARTICLE POTENTIALS

Consider a classical system of point particles, representing a fluid, and spherical clusters called nanoparticles. While in reality, a nanoparticle is a cluster of a number of atoms, here each nanoparticle will be modeled by a smooth internal density profile $\rho(x)$ that depends on the distance x from the center of the nanoparticle only and which is strictly zero for $x > s$, where s is the radius of the spherical nanoparticle. This approximation is motivated by the idea that for spherical nanoparticles, the inhomogeneities due to the discreteness of the atoms inside the nanoparticles should only have a small influence on the effective nanoparticle potentials. Given a density profile $\rho(x)$, one can make contact with the picture of a nanoparticle as a cluster of distinct atoms by interpreting $M = \int_{\mathcal{B}_s} d\mathbf{x} \rho(x)$ as the total number of atoms inside the nanoparticle, where $x = |\mathbf{x}|$, and \mathcal{B}_s denotes that the integration over \mathbf{x} is over the volume of a ball of radius s around zero.

To further illustrate that it is reasonable to smooth out the internal density, consider the idealized case that the atoms composing the nanoparticle are arranged in a face-centered-cubic (fcc) lattice—the crystal structure of e.g. aluminium, silver, gold, and platinum¹⁸—with one of the atoms in the center. The true density inside the nanoparticle is then a sum of delta functions, but this can be coarse-grained by taking a spherical shell of radius x with a width δx , counting the number of atoms in the shell, and dividing by the volume of the shell. The result of such coarse-graining is shown in Fig. 1 for a lattice with mean number density $\bar{\rho} = 1$ and for two values of the coarse-graining width, $\delta x = 3/4$ and $\delta x = 3/2$. The coarse-grained density around a single atom in an fcc crystal is seen to be reasonably constant except near the central atom (with the positive and negative deviations from the

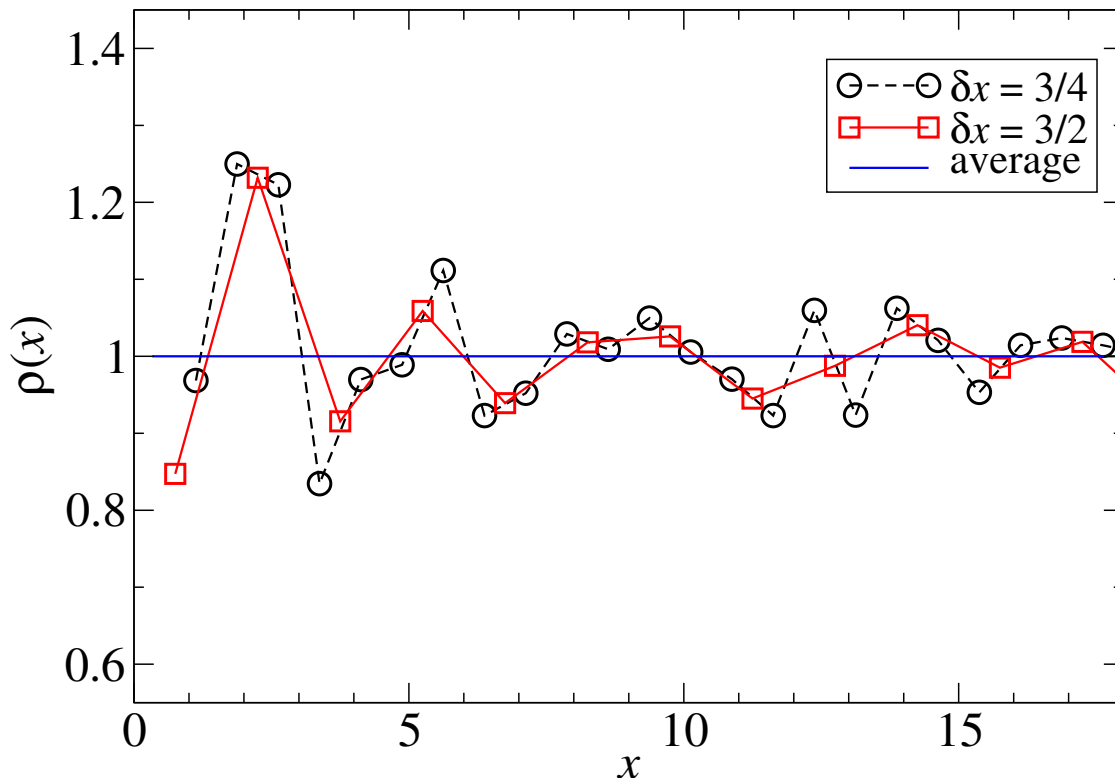


FIG. 1: Coarse-grained radial density profile of the fcc lattice of mean density $\bar{\rho} = 1$ as a function of the distance from a central atom. The circles correspond to a coarse-graining width of $\delta x = 3/4$, the squares corresponds to $\delta x = 3/2$ (the points are connected to guide the eye). The horizontal line indicates the mean number density.

mean density averaging out for larger δx), so that to first order the density may be replaced by a constant. This highly idealized nanoparticle structure will be used again in Sec. VI to get an idea of the accuracy of the effective potentials.

Let $\phi_{\text{pn}}(r)$ denote the basic pair potential between a point of a nanoparticle and a point particle in the fluid, where r is the distance between them. This potential will be assumed to be analytic for $r > 0$ but may diverge as $r \rightarrow 0$. The effective point-nanoparticle pair potential V_{pn} is then given by

$$V_{\text{pn}}(r) = \int_{\mathcal{B}_s} d\mathbf{x} \rho(x) \phi_{\text{pn}}(|\mathbf{r} - \mathbf{x}|), \quad (1)$$

where the subscript pn denotes that this is a point particle-nanoparticle potential and \mathbf{r} is the distance vector between the point particle and the center of the nanoparticle. Because of the spherical symmetry of the density profile and the pair potential ϕ_{pn} , the effective potential does not depend on the direction of \mathbf{r} , only on its magnitude $r = |\mathbf{r}|$.

Analogously, the effective inter-nanoparticle potential V_{nn} for two nanoparticles with internal density profiles ρ_1 and ρ_2 , radii s_1 and s_2 , and whose points interact through a pair potential ϕ_{nn} , is given by

$$V_{\text{nn}}(r) = \int_{\mathcal{B}_{s_1}} d\mathbf{x} \int_{\mathcal{B}_{s_2}} d\mathbf{y} \rho_1(x) \rho_2(y) \phi_{\text{nn}}(|\mathbf{r} - \mathbf{x} - \mathbf{y}|), \quad (2)$$

The potential ϕ_{nn} will also be assumed to be analytic for $r > 0$. Throughout this paper, ϕ_{pn} and ϕ_{nn} will be referred to as the *basic pair potentials*, while V_{pn} and V_{nn} are the *effective potentials*.

To arrive at more concrete expressions for the effective potentials, it will be assumed that the internal density profile of the nanoparticles is analytic, so that it may be written as a Taylor series,

$$\rho(x) = \Theta(s - x) \sum_{\substack{i=0 \\ i \text{ even}}}^{\infty} a_i x^i, \quad (3)$$

where Θ is the Heaviside step function. In Eq. (3), odd powers of x were omitted since they lead to non-analytic behavior at $x = 0$. The potentials for a nanoparticle and a point particle, and for two nanoparticles, respectively, that would result from internal densities of monomial form $\Theta(s - x)x^i$ are denoted by

$$V_i(r) = \int_{B_s} d\mathbf{x} x^i \phi_{\text{pn}}(|\mathbf{r} + \mathbf{x}|), \quad (4)$$

$$V_{ij}(r) = \int_{B_{s_1}} d\mathbf{x} \int_{B_{s_2}} d\mathbf{y} x^i y^j \phi_{\text{nn}}(|\mathbf{r} + \mathbf{x} - \mathbf{y}|). \quad (5)$$

Here, and below, the dependence of V_i and V_{ij} on s and s_1 and s_2 will not be denoted explicitly. In terms of the potentials V_i and V_{ij} , the effective point-nanoparticle and inter-nanoparticle potentials are given by

$$V_{\text{pn}}(r) = \sum_{\substack{i=0 \\ i \text{ even}}}^{\infty} a_i V_i(r) \quad (6)$$

$$V_{\text{nn}}(r) = \sum_{\substack{i=0 \\ i \text{ even}}}^{\infty} \sum_{\substack{j=0 \\ j \text{ even}}}^{\infty} a_i b_j V_{ij}(r) \quad (7)$$

where $\rho_1(x) = \Theta(s_1 - x) \sum_i a_i x^i$ and $\rho_2(x) = \Theta(s_2 - x) \sum_j b_j x^j$ are the internal density profiles of two interacting nanoparticles. While often only the first term $i = j = 0$ will suffice, the formalism will be developed for general i and j , since this is not any more difficult.

The three-dimensional and six-dimensional integrals in Eqs. (4) and (5) for the effective potentials make further manipulations cumbersome. However, due to the spherical symmetry of the basic pair potentials, these multi-dimensional integrals can be rewritten as integrals over a single variable.

To convert Eq. (4) to a single integral, one goes over to spherical coordinates $\mathbf{x} = (x \sin \theta \cos \varphi, x \sin \theta \sin \varphi, x \cos \theta)$, integrates over φ and then performs a change of integration variable from θ to $y = [x^2 \sin^2 \theta + (r - x \cos \theta)^2]^{1/2}$, which yields

$$V_i(r) = \frac{2\pi}{r} \int_0^s dx \int_{|r-x|}^{r+x} dy x^{i+1} y \phi_{\text{pn}}(y),$$

Reversing the order of the x and y integrals and using that i is even leads to

$$V_i(r) = \frac{2\pi}{(i+2)r} \left[\int_{|r-s|}^{r+s} dy [s^{i+2} - (r-y)^{i+2}] y \phi_{\text{pn}}(y) \right. \\ \left. + \Theta(s-r) \int_0^{s-r} dy [(r+y)^{i+2} - (r-y)^{i+2}] y \phi_{\text{pn}}(y) \right]. \quad (8)$$

Defining a kernel

$$K_i(x, s) = \frac{2\pi}{i+2} (s^{i+2} - x^{i+2}) \Theta(s - |x|), \quad (9)$$

one can write the right hand side of Eq. (8) in the concise form

$$V_i(r) = \frac{1}{r} \int dy K_i(r - y, s) y \phi_{\text{pn}}(|y|), \quad (10)$$

at least for $r > s$. That Eq. (10) also holds for $r < s$ (with the same expression for K_i) is seen by writing the second term in Eq. (8) as

$$\begin{aligned} & \int_0^{s-r} dy [\{s^{i+2} - (r-y)^{i+2}\} - \{s^{i+2} - (r+y)^{i+2}\}] y \phi_{\text{pn}}(y) \\ &= \int_{-s+r}^{s-r} dy [s^{i+2} - (r-y)^{i+2}] y \phi_{\text{pn}}(|y|). \end{aligned}$$

Combining this with the first term in Eq. (8) leads again to Eq. (10). Note that for the special case of $i = 0$, to be used below, the kernel takes the form

$$K_0(x, s) = \pi(s^2 - x^2) \Theta(s - |x|). \quad (11)$$

For the effective inter-nanoparticle potential V_{ij} , one can use that the potential energy of two nanoparticles is equivalent to the potential energy of a particle and a nanoparticle of which the points interact via a point-nanoparticle potential V_j , i.e.,

$$V_{ij}(r) = \frac{1}{r} \int dy K_i(r - y, s_1) y V_j(|y|),$$

where in V_j , one should replace s by s_2 , and ϕ_{pn} by ϕ_{nn} . Combining this with Eq. (10), and using that $K_j(x, s_2)$ is even in x , one obtains

$$V_{ij}(r) = \frac{1}{r} \int dy dz K_i(r - y, s_1) K_j(y - z, s_2) z \phi_{\text{nn}}(|z|), \quad (12)$$

or

$$V_{ij}(r) = \frac{1}{r} \int dy K_{ij}(r - y, s_1, s_2) y \phi_{\text{nn}}(|y|), \quad (13)$$

with the kernel K_{ij} given by

$$K_{ij}(x, s_1, s_2) = \int dy K_i(x - y, s_1) K_j(y, s_2). \quad (14)$$

The integral in this expression is further evaluated in the Appendix, where it is shown that K_{ij} is a piecewise polynomial function of degree $i + j + 5$ which has a finite support $|x| \leq s_1 + s_2$, and non-analytic points at $x = \pm|s_1 - s_2|$. For the special case $i = j = 0$ which will be used below, one finds from Eqs. (A3) and (A4), and after some rewriting,

$$K_{00}(x, s_1, s_2) = \begin{cases} \frac{\pi^2}{30} (D - |d|)^3 (d^2 + 3D|d| + D^2 - 5x^2) & 0 \text{ if } |x| \leq |d| \\ \frac{\pi^2}{30} (D - |x|)^3 (x^2 + 3D|x| + D^2 - 5d^2) & \text{if } |d| < |x| \leq D \\ 0 & \text{if } |x| > D, \end{cases} \quad (15)$$

where

$$\begin{aligned} D &= s_1 + s_2 \\ d &= s_1 - s_2. \end{aligned} \tag{16}$$

Because the kernels K_i and K_{ij} are piecewise polynomials, the integrals in Eqs. (10) and (13) can be performed analytically for many functional forms of ϕ_{pn} and ϕ_{nn} , such as power law and exponential forms (see Sec. V), which are the basis of many commonly used empirical pair potentials.

III. AUXILIARY POTENTIALS

Although not evident from Eqs. (10) and (13), the non-analytic points of the kernels and of the basic pair potential cause the effective potentials to have different functional forms depending on whether there is overlap. Different overlapping cases can occur: A point particle and a nanoparticle can either overlap (for $r < s$) or not overlap (for $r > s$), while two nanoparticles can have no overlap, which requires $r > s_1 + s_2 = D$, or partially overlap, or the smallest nanoparticle can be completely embedded in the larger, which occurs when $r < |s_1 - s_2| = |d|$. The different forms of the effective potentials for these different cases can be linked by introducing auxiliary potentials.

The following symmetrization operations on functions f are useful in denoting the relations between effective and auxiliary potentials:²¹

$$\begin{aligned} f([x]) &= f(x) - f(-x) \text{ “antisymmetrization”} \\ f((x)) &= f(x) + f(-x) \text{ “symmetrization.”} \end{aligned}$$

These operations are also useful for functions with multiple arguments, e.g.,

$$\begin{aligned} f([x], y) &= f(x, y) - f(-x, y) \\ f(x, (y)) &= f(x, y) + f(x, -y) \\ f([x], [y]) &= f(x, y) - f(-x, y) - f(x, -y) + f(-x, -y) \\ f([x, y]) &= f(x, y) - f(-x, -y). \end{aligned}$$

Note that in the last example, a single antisymmetrization was performed which involved both arguments.

The expressions of the effective potentials V_i and V_{ij} in terms of auxiliary potentials (whose derivations will follow) are given by

$$V_i(r) = \begin{cases} A_i((r), s) & \text{if } r < s \\ A_i(r, [s]) & \text{if } r > s \end{cases} \tag{17}$$

$$V_{ij}(r) = \begin{cases} A_{ij}((r), [s_1], s_2) & \text{if } r < |d| \text{ and } s_1 < s_2 \\ A_{ij}((r), s_1, [s_2]) & \text{if } r < d \text{ and } s_1 > s_2 \\ A_{ij}((r), s_1, s_2) - A_{ij}(r, (s_1, -s_2)) & \text{if } |d| < r < D \\ A_{ij}(r, [s_1], [s_2]) & \text{if } r > D, \end{cases} \tag{18}$$

in which the auxiliary potentials are defined as

$$A_i(r, s) = \frac{1}{r} \int_0^{r+s} dy \bar{K}_i(r-y, s) y \phi_{\text{pn}}(y) \tag{19}$$

$$A_{ij}(r, s_1, s_2) = \frac{1}{r} \int_0^{r+s_1+s_2} dy \bar{K}_{ij}(r-y, s_1, s_2) y \phi_{\text{nn}}(y), \tag{20}$$

where furthermore

$$\bar{K}_i(x, s) = \frac{2\pi}{i+2} (s^{i+2} - x^{i+2}) \quad (21)$$

$$\bar{K}_{ij}(x, s_1, s_2) = \int_{-s_2}^{x+s_1} dy \bar{K}_i(x-y, s_1) \bar{K}_j(y, s_2). \quad (22)$$

Note that \bar{K}_i is the analytic continuation of K_i , while the quantity $\bar{K}_{ij}(x, s_1, s_2)$ has the same functional form as the kernel K_{ij} for $x < 0$, $d < |x| < D$ (as it coincides with case 4 in the appendix). In particular, for $i = j = 0$, one has from Eq. (15)

$$\bar{K}_{00}(x, s_1, s_2) = \frac{\pi^2}{30} (s_1 + s_2 + x)^3 (x^2 - 3s_1x - 3s_2x - 4s_1^2 - 4s_2^2 + 12s_1s_2). \quad (23)$$

The derivation of Eq. (17) goes as follows. Consider first the non-overlapping case $r > s$. In that case, the absolute value sign in the argument of ϕ_{pn} may be dropped in Eq. (10), since $r > s$ and $r - y < s$ [cf. Eq. (9)] imply that $y > 0$. Thus, the effective point-nanoparticle potential can be written as

$$\begin{aligned} V_i(r) &= \frac{1}{r} \int dy K_i(r-y, s) y \phi_{\text{pn}}(y) \\ &= \frac{1}{r} \int_{r-s}^{r+s} dy \bar{K}_i(r-y, s) y \phi_{\text{pn}}(y) \\ &= \frac{1}{r} \int_0^{r+s} dy \bar{K}_i(r-y, s) y \phi_{\text{pn}}(y) + \frac{1}{r} \int_{r-s}^0 dy \bar{K}_i(r-y, s) y \phi_{\text{pn}}(y) \\ &= A_i(r, s) - A_i(r, -s) \\ &= A_i(r, [s]), \end{aligned} \quad (24)$$

For the case $r < s$, the argument in the ϕ_{pn} function in Eq. (10) needs to be $-y$ for $y < 0$, giving

$$\begin{aligned} V_i(r) &= \frac{1}{r} \int_0^{r+s} dy \bar{K}_i(r-y, s) y \phi_{\text{pn}}(y) + \frac{1}{r} \int_{r-s}^0 dy \bar{K}_i(r-y, s) y \phi_{\text{pn}}(-y) \\ &= \frac{1}{r} \int_0^{r+s} dy \bar{K}_i(r-y, s) y \phi_{\text{pn}}(y) - \frac{1}{r} \int_0^{s-r} dy \bar{K}_i(-r-y, s) y \phi_{\text{pn}}(y), \end{aligned} \quad (25)$$

where a change of integration variable from y to $-y$ was carried out in the second integral, and it was used that $\bar{K}_i(y, s)$ is even in y . The first term on the right hand side of Eq. (25) is equal to $A_i(r, s)$ in Eq. (19), while the second term equals $A_i(-r, s)$, so that

$$V_i(r) = A_i(r, s) + A_i(-r, s) \equiv A_i((r), s). \quad (26)$$

Thus, although the effective potentials between a point particle and a nanoparticle have different forms for non-overlapping and overlapping situations [Eqs. (24) and (26), respectively], both can be written in terms of the auxiliary potential A_i , and one obtains Eq. (17).

A technical difficulty must be mentioned here, namely, that the integral defining the auxiliary potential in Eq. (19) may not converge, even when the linear combinations in Eq. (17) do. In such cases, one should strictly write the auxiliary potential as a sum of a regular and a diverging part by replacing the lower limit of the integral in Eq. (19) by $\delta > 0$, and expanding the result in δ . In the absence of overlap, Eq. (17) must yield a finite result,

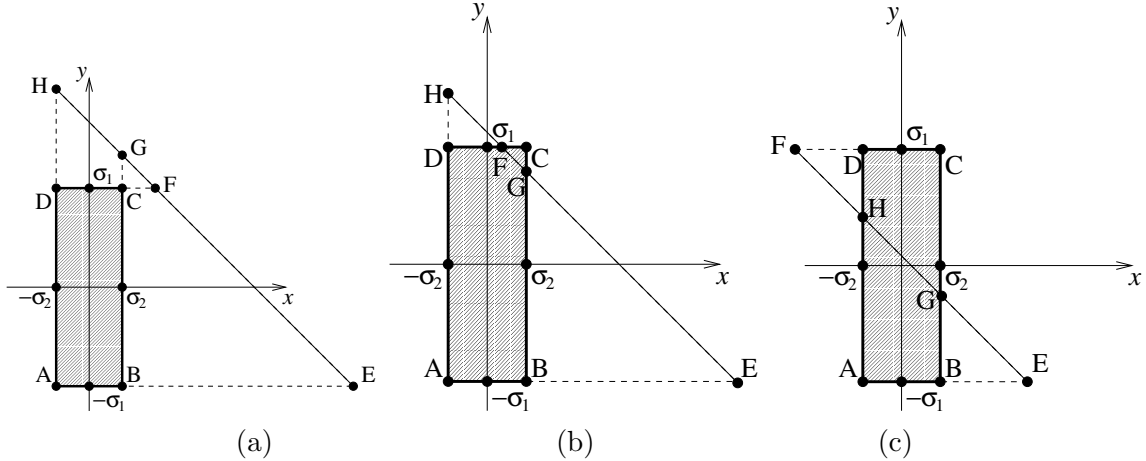


FIG. 2: Subdivision of the integration domain in the derivation of the expression of the inter-nanoparticle effective potential V_{ij} in terms of the auxiliary potential A_{ij} . Assuming $s_1 > s_2$, three cases have been distinguished: (a) $r > s_1 + s_2$, (b) $s_1 - s_2 < r < s_1 + s_2$, and (c) $r < s_1 - s_2$.

i.e., the diverging parts (negative powers of δ and possibly logarithmic terms) must cancel, hence in that case it suffices to work with the regular part of the auxiliary potential. On the other hand, in case of overlap, it is possible that the divergent parts do not cancel in Eq. (26), resulting in infinite effective potentials. An independent criterion for whether an effective potential is infinite in overlapping cases can be constructed as follows. For a single particle inside a nanoparticle, the effective potential becomes infinite only if the divergence of the basic pair potential ϕ_{pn} at the origin is too strong. In particular, if $\phi(r) \propto r^{-k}$ for small r then the point-nanoparticle potential is infinite for $k \geq 3$, as is seen by considering a small sphere around the particle, giving an integral of the form $\int_{r<\delta} \mathbf{dr} \phi(r) \propto \int_0^\delta dr r^2 r^{-k} \sim \frac{\delta^{3-k}}{3-k}$, which diverges for $k \geq 3$ in the limit $\delta \rightarrow 0$. This result extends to inter-nanoparticle potentials, which are also infinite if there is overlap and the potential ϕ_{nn} diverges no slower than r^{-3} , i.e., the $V_{ij}(r)$ are finite for $r < D$ provided $\phi_{\text{nn}}(r)$ diverges for small r slower than r^{-3} . Given this criterion, the divergent part of an auxiliary potential is not needed to determine whether the corresponding effective potential is infinite. Since the divergent parts are needed neither in overlapping nor in non-overlapping cases, below, only the regular parts of auxiliary potentials will be given.

To derive Eq. (18) for the effective potentials between two nanoparticles, one starts by rewriting Eq. (12) to

$$V_{ij}(r) = \frac{1}{r} \int_{-s_1}^{s_1} dy \int_{-s_2}^{s_2} dx \bar{K}_i(y, s_1) \bar{K}_j(x, s_2) (r - x - y) \phi_{\text{nn}}(|r - x - y|). \quad (27)$$

In this formulation, the integration domain is a rectangle in the (x, y) plane and the integrand has a diagonal non-analytic line at $x + y = r$. This line may or may not cross the domain, which is what gives rise to non-analyticity and the difference between overlapping and non-overlapping effective potentials.

Subdividing the domain into triangular regions without non-analyticities will result in expressions in terms of analytic subexpressions. The appropriate subdivisions of the integration domain are shown in Fig. 2, where it was assumed that the radius s_1 is larger than the radius s_2 . The three panels of the figure correspond to the three cases that need to be distinguished: (a) no overlap: $r > s_1 + s_2$, (b) partial overlap: $s_1 - s_2 < r < s_1 + s_2$, and (c)

complete overlap, $r < s_1 - s_2$. In all three panels of Fig. 2, the rectangle ABCD is the integration domain, and the diagonal line through points E and H is the line of non-analyticities (where $r - x - y = 0$). For points below this line, the absolute value in the argument of ϕ_{nn} in Eq. (27) may be omitted, while for points above this line, it changes the sign of the argument. Considering first case (a), i.e., no overlap, one sees from Fig. 2(a) that

$$V_{ij}(r) = I_{\text{AEH}}^+ - I_{\text{BEG}}^+ - I_{\text{DFH}}^+ + I_{\text{CFG}}^+, \quad (28)$$

where I_{XYZ}^+ is the integral (27) with the absolute value sign omitted, and evaluated over the area of the triangle XYZ. For case (b), i.e., partial overlap, one finds from Fig. 2(b)

$$V_{ij}(r) = I_{\text{AEH}}^+ - I_{\text{BEG}}^+ - I_{\text{DFH}}^+ + I_{\text{CFG}}^-, \quad (29)$$

where the superscript “-” indicates that the sign of the argument of ϕ_{nn} in Eq. (27) is changed. Finally for case (c), one finds from Fig. 2(c)

$$V_{ij}(r) = I_{\text{AEH}}^+ - I_{\text{BEG}}^+ - I_{\text{DFH}}^- + I_{\text{CFG}}^-. \quad (30)$$

Note that for even basic potentials ϕ_{pn} and ϕ_{nn} , the sign of the arguments is inconsequential, so that all three cases (28)–(30) will have the same functional form.

The integration limits appropriate for the triangular regions are easily determined from Fig. 2. This yields the following explicit expression for the integral I_{AEH}^+ :

$$\begin{aligned} I_{\text{AEH}}^+ &= \frac{1}{r} \int_{-s_2}^{r+s_1} dx \int_{-s_1}^{r-x} dy \bar{K}_i(y, s_1) \bar{K}_j(x, s_2) (r - x - y) \phi_{\text{nn}}(r - x - y) \\ &= A_{ij}(r, s_1, s_2). \end{aligned} \quad (31)$$

Here, the identification with A_{ij} followed from Eqs. (20) and (22). Given the form of the auxiliary potential in Eq. (31), it is not hard to show that

$$I_{\text{BEG}}^+ = A_{ij}(r, s_1, -s_2), \quad I_{\text{DFH}}^+ = A_{ij}(r, -s_1, s_2), \quad I_{\text{CFG}}^+ = A_{ij}(r, -s_1, -s_2), \quad (32)$$

so that with Eq. (28) one finds for the non-overlapping case

$$\begin{aligned} V_{ij}(r) &= A_{ij}(r, s_1, s_2) - A_{ij}(r, s_1, -s_2) - A_{ij}(r, -s_1, s_2) + A_{ij}(r, -s_1, -s_2) \\ &= A_{ij}(r, [s_1], [s_2]), \end{aligned} \quad (33)$$

As was the case for A_i , A_{ij} may have divergent parts which cancel in Eq. (33) and will be omitted below.

According to Eqs. (28) and (29), the partially overlapping case (b) only requires replacing I_{CFG}^+ by I_{CFG}^- , which is given by

$$I_{\text{CFG}}^- = \frac{1}{r} \int_{r-s_1}^{s_2} dx \int_{r-x}^{s_1} dy \bar{K}_i(y, s_1) \bar{K}_j(x, s_2) (r - x - y) \phi_{\text{nn}}(-r + x + y). \quad (34)$$

Substituting $y \rightarrow -y$, $x \rightarrow -x$, and using that \bar{K}_i and \bar{K}_j are even in x and y , one finds

$$I_{\text{CFG}}^- = A_{ij}(-r, s_1, s_2), \quad (35)$$

so that for $d < r < D$:

$$\begin{aligned} V_{ij}(r) &= A_{ij}(r, s_1, s_2) - A_{ij}(r, s_1, -s_2) - A_{ij}(r, -s_1, s_2) + A_{ij}(-r, s_1, s_2) \\ &= A_{ij}((r), s_1, s_2) - A_{ij}(r, (s_1, -s_2)) \end{aligned} \quad (36)$$

For the fully overlapping case, finally, one furthermore needs to replace I_{DFH}^+ by

$$\begin{aligned} I_{\text{DFH}}^- &= \frac{1}{r} \int_{r-s_1}^{-s_2} dx \int_{r-z}^{s_1} dy \bar{K}_i(y, s_1) \bar{K}_j(x, s_2) (r-x-y) \phi_{\text{nn}}(-r+x+y) \\ &= A_{ij}(-r, s_1, -s_2), \end{aligned} \quad (37)$$

whence for $r < d$:

$$\begin{aligned} V_{ij}(r) &= A_{ij}(r, s_1, s_2) - A_{ij}(r, s_1, -s_2) - A_{ij}(-r, s_1, -s_2) + A_{ij}(-r, s_1, s_2) \\ &= A_{ij}((r), s_1, [s_2]). \end{aligned} \quad (38)$$

The reason that this is not symmetric in s_1 and s_2 is because of the assumption that $s_1 > s_2$. With $s_1 < s_2$ and $r < s_2 - s_1$, one would have obtained $V_{ij}(r) = A_{ij}((r), [s_1], s_2)$. This completes the derivation of Eq. (18).

There is a degree of freedom in choosing the auxiliary potentials in Eqs. (17) and (18), since they enter only in specific combinations. In particular, according to Eq. (17), the effective point-nanoparticle potential is either r symmetric or s -antisymmetric. Thus, one may replace $A_i(r, s)$ by $A_i(r, s) + X(r, s)$ if the function $X(r, s)$ is antisymmetric in r as well as symmetric in s , i.e., if

$$X(r, s) = X(r, -s) = -X(-r, s). \quad (39)$$

Conversely, any terms in A_i that satisfy Eq. (39) are irrelevant to Eq. (17) and may, therefore, be omitted. Similarly, the effective inter-nanoparticle potential in Eq. (18) is not affected by adding a function $Y(r, s_1, s_2)$ to the auxiliary potential A_{ij} , as long as Y satisfies

$$\begin{aligned} Y(r, s_1, s_2) - Y(r, -s_1, s_2) - Y(r, s_1, -s_2) + Y(r, -s_1, -s_2) &= 0 \\ Y(r, s_1, s_2) &= Y(-r, -s_1, -s_2), \end{aligned} \quad (40)$$

while terms present in A_{ij} that satisfy these relations are irrelevant, and may be omitted.

IV. SOLID AND HOLLOW NANOPARTICLES

Two particular cases of the internal nanoparticle densities ρ will be considered in detail below. The first is a uniform internal density ρ inside a solid sphere of radius s :

$$\rho(x) = \rho \Theta(s - x). \quad (41)$$

Since Eq. (41) is of the form $a_i \Theta(s - x) x^i$ with $i = 0$ and $a_0 = \rho$, Eq. (6) gives for the effective point-nanoparticle potential

$$V_{\text{pn}}(r) = \rho V_0(r). \quad (42)$$

Similarly, the effective inter-nanoparticle potential of two solid nanoparticles of uniform density ρ_1 and ρ_2 , and radii s_1 and s_2 , respectively, satisfies [cf. Eq. (7)]

$$V_{\text{nn}}(r) = \rho_1 \rho_2 V_{00}(r). \quad (43)$$

The second type of “internal” density $\rho(x)$ considered here is that of hollow nanoparticles, whose density is concentrated on the surface of the sphere, i.e.,

$$\rho(x) = \tilde{\rho} \delta(s - x), \quad (44)$$

where $\tilde{\rho}$ is the surface density on the area of the sphere of size s . This density is appropriate to describe e.g. buckyballs.¹⁷ The density in Eq. (44) cannot be written in the form Eq. (3), but it is linked to the uniform internal density in Eq. (41) by

$$\tilde{\rho}\delta(s-x) = \tilde{\rho} \frac{\partial\Theta(s-x)}{\partial s}. \quad (45)$$

Consequently, the effective point-nanoparticle potential for this case is given by

$$V_{\text{pn}}(r) = \tilde{\rho} V_{\text{h}}(r), \quad (46)$$

with

$$V_{\text{h}}(r) = \frac{\partial V_0(r)}{\partial s}, \quad (47)$$

where the subscript h indicates that this potential acts between a hollow nanoparticle and a point particle.

In a similar fashion, the inter-nanoparticle potentials for a solid and a hollow nanoparticle (sh) is given by

$$V_{\text{nn}}(r) = \rho_1 \tilde{\rho}_2 V_{\text{sh}}(r) \quad (48)$$

and the potential for two hollow nanoparticles (hh) satisfies

$$V_{\text{nn}}(r) = \tilde{\rho}_1 \tilde{\rho}_2 V_{\text{hh}}(r), \quad (49)$$

where $\tilde{\rho}_1$ and $\tilde{\rho}_2$ are the surface density of the two nanoparticles, while the scaled inter-nanoparticle potentials in Eqs. (48)–(49) are given by

$$\begin{aligned} V_{\text{sh}}(r) &= \frac{\partial V_{00}(r)}{\partial s_2} \\ V_{\text{hh}}(r) &= \frac{\partial^2 V_{00}(r)}{\partial s_1 \partial s_2}. \end{aligned} \quad (50)$$

Thus, the effective potentials V_{h} , V_{sh} and V_{hh} can be found by differentiation once V_0 and V_{00} , are known.

The effective potentials for solid nanoparticles can be expressed in terms of auxiliary potentials A_0 and A_{00} using Eqs. (17) and (18). In applying Eqs. (47) and (50) to these expressions, it should be realized that taking a derivative turns an antisymmetrized function into a symmetrized one, and vice versa. Thus, by defining

$$\begin{aligned} A_{\text{h}}(r, s) &= \frac{\partial A_0(r, s)}{\partial s} \\ A_{\text{sh}}(r, s_1, s_2) &= \frac{\partial A_{00}(r, s_1, s_2)}{\partial s_2} \\ A_{\text{hh}}(r, s_1, s_2) &= \frac{\partial^2 A_{00}(r, s_1, s_2)}{\partial s_1 \partial s_2}, \end{aligned} \quad (51)$$

one gets for the effective potentials

$$V_{\text{h}}(r) = \begin{cases} A_{\text{h}}(r, s) & \text{if } r < s \\ A_{\text{h}}(r, s) & \text{if } r > s, \end{cases} \quad (52)$$

$$V_{\text{sh}}(r) = \begin{cases} A_{\text{sh}}((r), [s_1], s_2) & \text{if } r < |d| \text{ and } s_1 < s_2 \\ A_{\text{sh}}((r), s_1, (s_2)) & \text{if } r < d \text{ and } s_1 > s_2 \\ A_{\text{sh}}((r), s_1, s_2) + A_{\text{sh}}(r, [s_1, -s_2]) & \text{if } |d| < r < D \\ A_{\text{sh}}(r, [s_1], (s_2)) & \text{if } r > D, \end{cases} \quad (53)$$

$$V_{\text{hh}}(r) = \begin{cases} A_{\text{hh}}((r), (s_1), s_2) & \text{if } r < |d| \text{ and } s_1 < s_2 \\ A_{\text{hh}}((r), s_1, (s_2)) & \text{if } r < d \text{ and } s_1 > s_2 \\ A_{\text{hh}}((r), s_1, s_2) + A_{\text{hh}}(r, (s_1, -s_2)) & \text{if } |d| < r < D \\ A_{\text{hh}}(r, (s_1), (s_2)) & \text{if } r > D. \end{cases} \quad (54)$$

V. EFFECTIVE POTENTIALS FOR UNIFORMLY SOLID AND HOLLOW NANOPARTICLES

A. Power laws

Pair potentials of power law form

$$\phi^n(r) = \frac{1}{r^n}, \quad (55)$$

with n integer, are basic building blocks of many atomic and molecular pair potentials, such as the Coulomb potential ($n = 1$) and the Lennard-Jones potential (a linear combination of $n = 6$ and $n = 12$). Note that here and below, a superscript on a potential represents an index, not a power.

The effective potential V_0^n for a point particle and a solid nanoparticle of radius s whose points interact with the particle through $\phi_{\text{pn}} = \phi^n$ is given in terms of the auxiliary potential by Eq. (17). The auxiliary potential follows from Eqs. (19), giving, for general n ,

$$A_0^n(r, s) = \frac{\pi}{r} \int_0^{r+s} dy \frac{s^2 - (r-y)^2}{y^{n-1}} = \frac{2\pi[r + (n-3)s]}{(n-2)(n-3)(n-4)r(r+s)^{n-3}}, \quad (56)$$

where divergent terms were omitted, as explained in Sec. III.

The right hand side of Eq. (56) becomes ill-defined for the specific values $n = 2, 3$ and 4. This is caused by a term proportional to $x^{n'-n-1}$ in the integrand in Eq. (56) (with $n' = 2, 3$ or 4), which when $n = n'$ should have resulted in a term $\ln(r+s)$ instead of the erroneous and ill-defined expression $\frac{(r+s)^{n'-n}}{n'-n}$ that occurs in Eq. (56). Using that $\lim_{n \rightarrow n'} \frac{\partial}{\partial n} [(n-n') \frac{x^{n'-n}}{n'-n}] = \ln x$, this can be fixed by substituting

$$A^{n'} \longrightarrow \lim_{n \rightarrow n'} \frac{\partial}{\partial n} [(n-n')A^n]. \quad (57)$$

Applied to Eq. (56), this gives

$$\begin{aligned} A_0^2(r, s) &= \frac{\pi(r+s)(3r-s)}{2r} + \frac{\pi(s^2-r^2)}{r} \ln(r+s) \\ A_0^3(r, s) &= -\frac{2\pi s}{r} + 2\pi \ln(r+s) \\ A_0^4(r, s) &= -\frac{\pi(3r+s)}{2r(r+s)} - \frac{\pi}{r} \ln(r+s). \end{aligned} \quad (58)$$

The effective potential V_0^n is obtained from these expressions for the auxiliary potential using Eq. (17).

From Eqs. (51) and (56), it follows that the auxiliary potential for a hollow nanoparticle and a point particle is given by

$$A_h^n(r, s) = -\frac{2\pi s}{(n-2)r(r+s)^{n-2}}. \quad (59)$$

Equation (59) is ill-defined for $n = 2$, in which case one uses Eq. (57) to find

$$A_h^2(r, s) = \frac{2\pi s}{r} \ln(r+s). \quad (60)$$

The effective potential V_h^n is now obtained from Eq. (52).

For the effective inter-nanoparticle potential V_{00} , the auxiliary potential formulation (18) holds with $i = j = 0$, where the auxiliary potential is found using Eq. (20) with $\phi_{nn} = \phi^n$, giving

$$A_{00}^n(r, s_1, s_2) = \frac{4\pi^2 p_n(r, s_1, s_2)}{(n-7)(n-6)(n-5)(n-4)(n-3)(n-2)r(r+s_1+s_2)^{n-5}}, \quad (61)$$

where

$$p_n(r, s_1, s_2) = r^2 + (n-5)(s_1+s_2)r + (n-6)[s_1^2 + s_2^2 + (n-5)s_1s_2]. \quad (62)$$

The expression in Eq. (61) is ill-defined for $n = 2, 3, 4, 5, 6$ and 7 . Using again Eq. (57), the correct expression for A_{00}^n for these values of n is found to be

$$\begin{aligned} A_{00}^n(r, s_1, s_2) &= \frac{4\pi^2}{r(r+s_1+s_2)^{n-5} \prod_{\substack{\ell=2 \\ \ell \neq n}}^7 (\ell-n)} \\ &\times \left\{ p_n(r, s_1, s_2) \left[\ln(r+s_1+s_2) - \sum_{\substack{\ell=2 \\ \ell \neq n}}^7 \frac{1}{\ell-n} \right] \right. \\ &\quad \left. - s_1^2 - s_2^2 - (s_1+s_2)r + (11-2n)s_1s_2 \right\}. \quad (63) \end{aligned}$$

According to Eq. (51), the auxiliary potential for a solid sphere of radius s_1 and a hollow sphere of radius s_2 can be found by taking the derivative with respect to s_2 , yielding, for general n ,

$$A_{sh}^n(r, s_1, s_2) = \frac{-4\pi^2 s_2 [r + (n-4)s_1 + s_2]}{(n-5)(n-4)(n-3)(n-2)r(r+s_1+s_2)^{n-4}}. \quad (64)$$

Finally, the effective potential for two hollow spheres follows from another derivative with respect to s_1 [cf. Eq. (51)], leading to

$$A_{hh}^n(r, s_1, s_2) = \frac{4\pi^2 s_1 s_2}{(n-3)(n-2)r(r+s_1+s_2)^{n-3}}. \quad (65)$$

For the ill-defined cases of Eqs. (64) and (65), one can use Eq. (57) to get expressions similar to the one in Eq. (63).

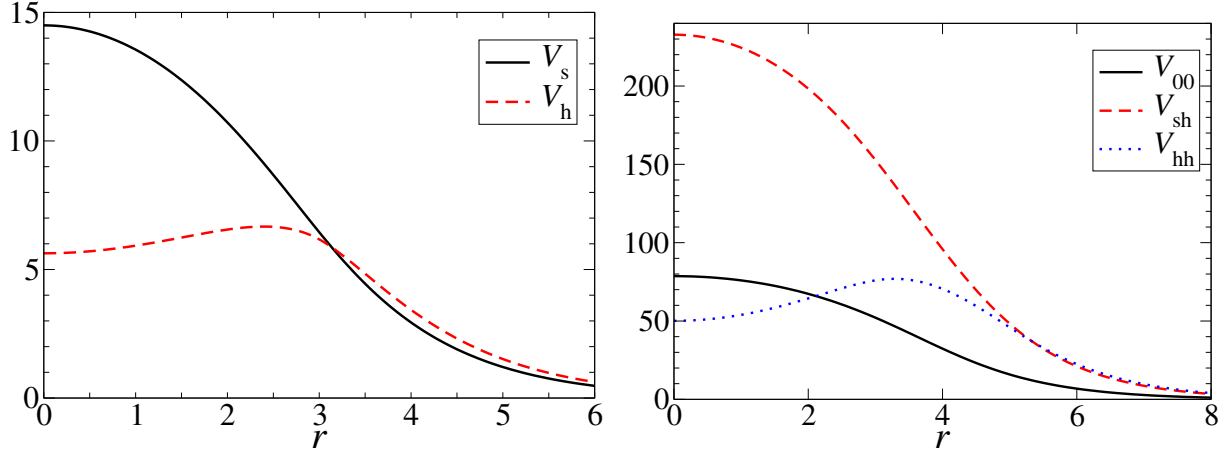


FIG. 3: Typical example of effective potentials based on an exponential interaction [Eqs. (18) and (69)]. The left panel shows the point-nanoparticle potentials for solid (s) and hollow (h) spheres with radius $s = 3$, while the right panel shows the inter-nanoparticle potentials for radii $s_1 = 4$ and $s_2 = 1$.

B. Exponentials

The effective interactions as a result of the exponential pair potential

$$\phi^E(r) = e^{-r} \quad (66)$$

will now be derived. Substituting this potential for ϕ_{pn} in the expression (19) for the auxiliary potential gives

$$A_0^E(r, s) = \frac{2\pi(3 + r + sr + s^2 + 3s)}{r} e^{-r-s} + 4\pi, \quad (67)$$

where an irrelevant expression satisfying Eq. (39) was omitted. From Eqs. (51) and (67), the auxiliary potential for a point particle and a hollow nanoparticle is found to be

$$A_h^E(r) = -\frac{2\pi s(1 + r + s)}{r} e^{-r-s}. \quad (68)$$

Note that the corresponding effective potentials follow from Eqs. (17) and (52).

The effective inter-nanoparticle potential is of the auxiliary potential form (18) with $i = j = 0$. The auxiliary potential A_{00}^E is found using Eq. (20) with $\phi_{\text{nn}} = \phi^E$, giving

$$A_{00}^E(r, s_1, s_2) = 4\pi^2 \frac{(r + s_1 + s_2 + 5)(s_1 + 1)(s_2 + 1) + 1 - s_1 s_2}{r} e^{-r-s_1-s_2} + \frac{\pi^2}{3r} \left[8(s_1 + s_2)(s_1^2 + s_2^2 - s_1 s_2)r + 6(s_1^2 + s_2^2 - 4)(r^2 + 4) - r^4 + 3(s_1^2 - s_2^2)^2 + 24 \right] \quad (69)$$

where an expression satisfying Eq. (40) has been omitted. Using Eqs. (51), the auxiliary potential for the interaction between a solid and a hollow nanoparticle and between two

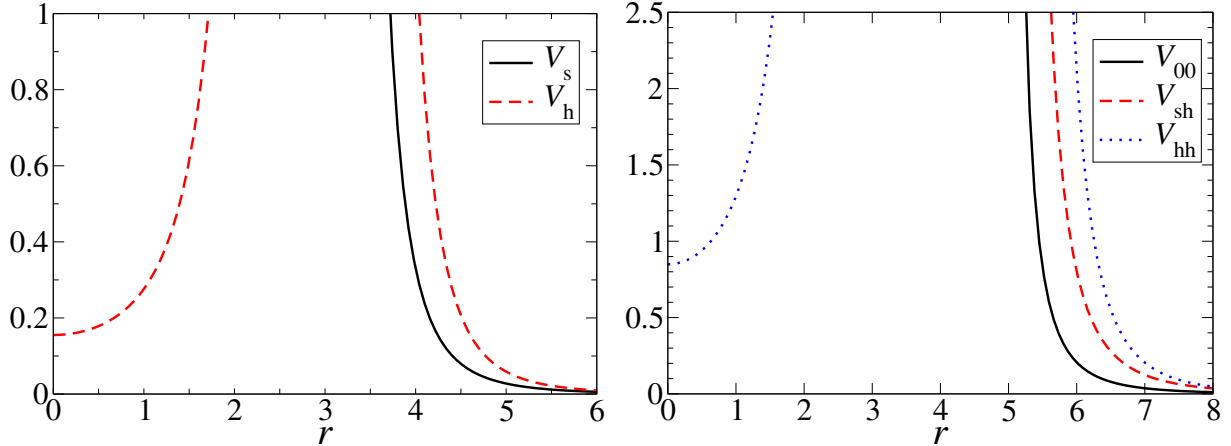


FIG. 4: Typical example of effective potentials based on the London-van der Waals interaction, i.e., the power law in Eq. (55) with $n = 6$. The left panel shows the potential for a point particle and solid or hollow nanoparticle of radius $s = 3$, the right panel shows the potential for two nanoparticles of radius $s_1 = 4$ and $s_2 = 1$.

hollow particles are found to be

$$A_{\text{sh}}^{\text{E}}(r, s_1, s_2) = \frac{-4\pi^2 s_2 [(r + s_1 + s_2 + 4)(s_1 + 1) - s_1]}{r} e^{-r-s_1-s_2} + \frac{4\pi^2 s_2 [(r + s_2)^2 - s_1^2 + 4]}{r} \quad (70)$$

$$A_{\text{hh}}^{\text{E}}(r, s_1, s_2) = \frac{4\pi^2 s_1 s_2 (r + s_1 + s_2 + 2)}{r} e^{-r-s_1-s_2} - \frac{8\pi^2 s_1 s_2}{r}. \quad (71)$$

Figure 3 shows a typical example of the effective potentials derived from the exponential basic potential [cf. Eqs. (17), (18), (52)–(54) and (67)–(71)]. One sees that these effective potentials are very smooth and do not have a hard core, which is typical for effective potentials based on a basic pair potential that does not diverge for small distances.

C. Examples using common pair potentials

London-van der Waals potential

In this section, the effective potentials based on the London-van der Waals potential

$$\phi^6(r) = \frac{1}{r^6} \quad (72)$$

will be presented. Note that the negative prefactor that occurs in front of the attractive London-van der Waals interaction has been omitted here. Substituting $n = 6$ into Eq. (56), and using Eq. (17), one finds the London-van der Waals potential for a solid nanoparticle and a point particle:

$$V_0^6(r) = \frac{4\pi s^3}{3(r^2 - s^2)^3}, \quad (73)$$

for $r > s$. This effective potential becomes infinite for $r < s$. For the London-van der Waals interaction of a hollow nanoparticle with a point particle, Eqs. (52) and (59) with $n = 6$, lead to

$$V_h^6(r) = \frac{4\pi s^2}{(r^2 - s^2)^3} + \frac{8\pi s^4}{(r^2 - s^2)^4}. \quad (74)$$

The effective London-van der Waals interaction potential for two solid nanoparticles is determined by substituting $n = 6$ into Eq. (63), and using Eq. (18), which gives

$$V_{00}^6(r) = \frac{\pi^2 s_1 s_2}{3(r^2 - d^2)} + \frac{\pi^2 s_1 s_2}{3(r^2 - D^2)} + \frac{\pi^2}{6} \ln \frac{r^2 - D^2}{r^2 - d^2}. \quad (75)$$

This result coincides with that of Hamaker.¹⁶

Using Eqs. (50) and (75), or using Eqs. (64) and (53), one finds for the London-van der Waals potential V_{sh}^6 for a solid nanoparticle of radius s_1 and a hollow nanoparticle of radius s_2

$$V_{sh}^6(r) = \frac{2\pi^2 s_1 s_2 D}{3(r^2 - D^2)^2} - \frac{2\pi^2 s_1 s_2 d}{3(r^2 - d^2)^2} - \frac{\pi^2 s_2}{3(r^2 - D^2)} + \frac{\pi^2 s_2}{3(r^2 - d^2)}. \quad (76)$$

The effective London-van der Waals potential V_{hh}^6 for two hollow nanoparticles, finally, is obtained from Eq. (76) using Eq. (50), or alternatively from Eqs. (65) and (54), with the result

$$V_{hh}^6(r) = \frac{8\pi^2 s_1 s_2 D^2}{3(r^2 - D^2)^3} - \frac{8\pi^2 s_1 s_2 d^2}{3(r^2 - d^2)^3} + \frac{2\pi^2 s_1 s_2}{3(r^2 - D^2)^2} - \frac{2\pi^2 s_1 s_2}{3(r^2 - d^2)^2}. \quad (77)$$

Figure 4 shows a typical example of the effective potentials for the London-van der Waals interaction as the basic pair potential.

Morse potential

The Morse potential²⁴

$$\phi^M(r) = e^{-2b(r-1)} - 2e^{-b(r-1)}, \quad (78)$$

is used e.g. for molecular bonds and for pure metals.²⁵ It is a sum of two exponential functions, so having derived the formulas for the exponential potential in Sec. VB, one easily finds the corresponding point-nanoparticle interactions by taking the combinations

$$V_0^M(r) = \frac{e^{2b}}{2^3 b^3} V_0^E(2br, 2bs) - \frac{2e^b}{b^3} V_0^E(br, bs) \quad (79)$$

$$V_h^M(r) = \frac{e^{2b}}{2^2 b^2} V_h^E(2br, 2bs) - \frac{2e^b}{b^2} V_h^E(br, bs), \quad (80)$$

where the notation $V_0^E(\alpha r, \beta s)$ indicates that in V_0^E and V_h^E , r is to be replaced by αr and s by βs . Likewise, the inter-nanoparticle interactions for the Morse potential in Eq. (78) are given by

$$V_{00}^M(r) = \frac{e^{2b}}{2^6 b^6} V_{00}^E(2br, 2bs_1, 2bs_2) - \frac{2e^b}{b^6} V_{00}^E(br, bs_1, bs_2). \quad (81)$$

$$V_{sh}^M(r) = \frac{e^{2b}}{2^5 b^5} V_{sh}^E(2br, 2bs_1, 2bs_2) - \frac{2e^b}{b^5} V_{sh}^E(br, bs_1, bs_2). \quad (82)$$

$$V_{hh}^M(r) = \frac{e^{2b}}{2^4 b^4} V_{hh}^E(2br, 2bs_1, 2bs_2) - \frac{2e^b}{b^4} V_{hh}^E(br, bs_1, bs_2). \quad (83)$$

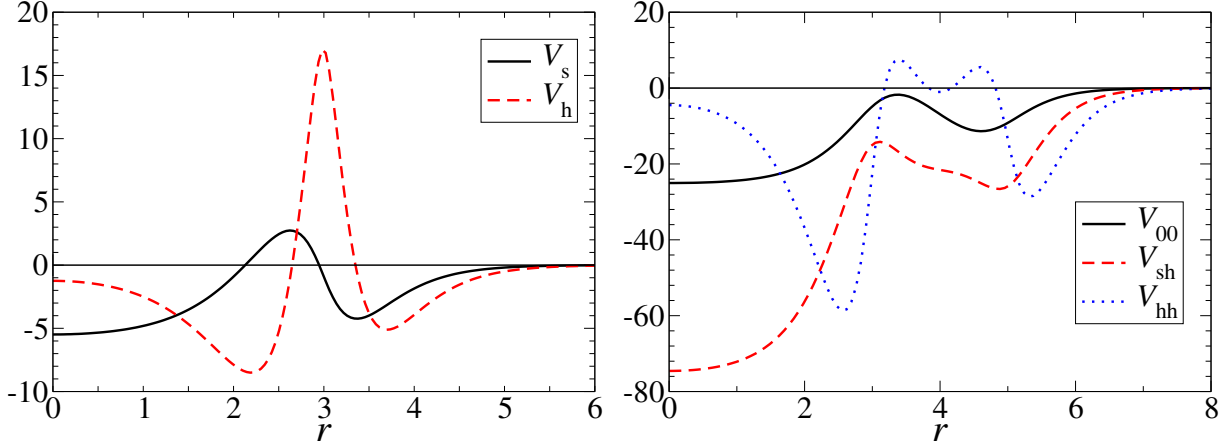


FIG. 5: Example of Morse effective potentials for $b = 2.6$. The left panel shows the effective potential for a particle and a solid or hollow nanoparticle of radius $s = 3$, the right panel shows the effective potentials for two nanoparticles of radius $s_1 = 4$ and $s_2 = 1$.

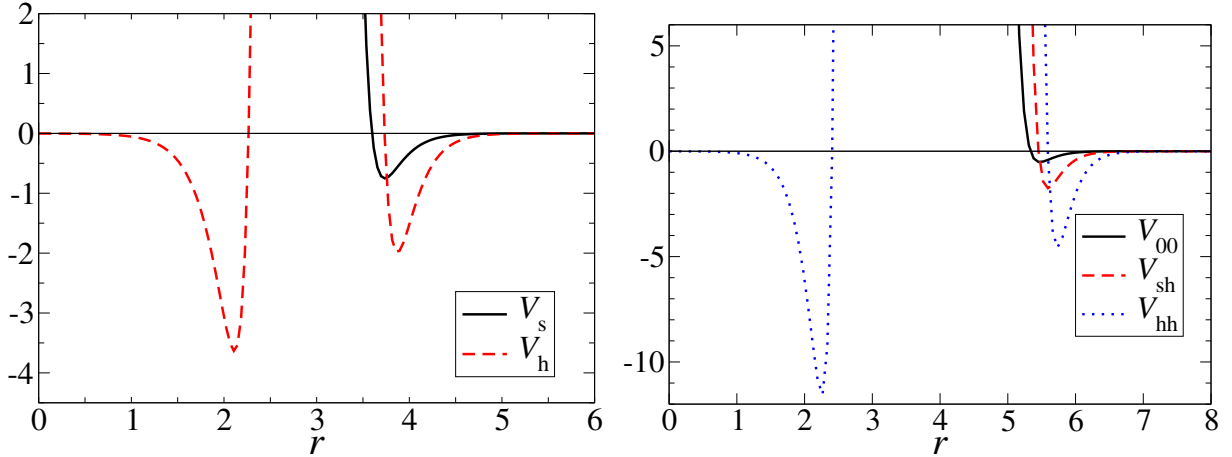


FIG. 6: Example of Morse effective potentials for $b = 5.6$, for which the Morse potential resembles the Lennard-Jones potential. The left panel shows the effective point-nanoparticle potentials for $s = 3$, the right panel shows the effective potentials for two nanoparticles of radius $s_1 = 4$ and $s_2 = 1$. Note that V_{sh} and V_{hs} are nearly the same for $r > D$.

Two examples of the Morse-based effective potentials are shown in Figs. 5 and 6, for $b = 2.6$ and $b = 5.6$, respectively. For the lower value of b , there is a low barrier for a point particle to penetrate a nanoparticle as well as for one nanoparticle to penetrate another (cf. Fig. 5), while for the larger value of b this is virtually impossible (cf. Fig. 6) if the energies of the particles are of order 1.

Buckingham potential

The modified Buckingham potential²⁶

$$\phi^{\text{B}}(r) = \begin{cases} \infty & \text{if } r < r^*, \\ ae^{-br} - cr^{-6} & \text{if } r > r^*, \end{cases} \quad (84)$$

is made up of an exponential part, for which the results of Sec. V B apply, and an attractive London-van der Waals term treated above. In addition, one needs to take the cut-off r^* into account. This cut-off is necessary because otherwise, for small enough r , the Buckingham potential would become negative. Thus, the effective point-nanoparticle potentials are

$$V_0^{\text{B}}(r) = \begin{cases} \infty & \text{if } r < s + r^* \\ \frac{a}{b^3} V_0^{\text{E}}(br, bs) - cV_0^6(r) & \text{if } r > s + r^* \end{cases} \quad (85)$$

$$V_{\text{h}}^{\text{B}}(r) = \begin{cases} \frac{a}{b^2} V_{\text{h}}^{\text{E}}(br, bs) - cV_{\text{h}}^6(r) & \text{if } r < s - r^* \\ \infty & \text{if } |s - r| < r^* \\ \frac{a}{b^2} V_{\text{h}}^{\text{E}}(br, bs) - cV_{\text{h}}^6(r) & \text{if } r > s + r^* \end{cases} \quad (86)$$

while the effective inter-nanoparticle potentials are given by

$$V_{00}^{\text{B}}(r) = \begin{cases} \infty & \text{if } r < D + r^* \\ \frac{a}{b^6} V_{00}^{\text{E}}(br, bs_1, bs_2) - cV_{00}^6(r) & \text{otherwise} \end{cases} \quad (87)$$

$$V_{\text{sh}}^{\text{B}}(r) = \begin{cases} \infty & \text{if } -d - r^* < r < D + r^* \\ \frac{a}{b^5} V_{\text{sh}}^{\text{E}}(br, bs_1, bs_2) - cV_{\text{sh}}^6(r) & \text{otherwise} \end{cases} \quad (88)$$

$$V_{\text{hh}}^{\text{B}}(r) = \begin{cases} \infty & \text{if } |d| - r^* < r < D + r^* \\ \frac{a}{b^4} V_{\text{hh}}^{\text{E}}(br, bs_1, bs_2) - cV_{\text{hh}}^6(r) & \text{otherwise.} \end{cases} \quad (89)$$

While the effective potentials due to the exponential pair potential are different for different cases (no overlap, partial overlap, and complete overlap), because of the presence of a cut-off r^* , only the non-overlapping case is relevant here.

In Fig. 7, a typical example of these potentials is shown. Note that while it is possible for a point or nanoparticle particle to be inside the hollow nanoparticle (as long as there is no overlap), there is an infinite barrier to get inside from the outside, in contrast with the effective potentials based on the Morse potential.

Lennard-Jones potential

One of the most often used potentials in molecular dynamics simulations is the Lennard-Jones potential,²² which in reduced units reads

$$\phi^{\text{LJ}}(r) = \frac{1}{r^{12}} - \frac{2}{r^6} = \phi^{12}(r) - 2\phi^6(r). \quad (90)$$

Since the attractive part of the Lennard-Jones potential in Eq. (90) was handled above, one only needs to add the repulsive part r^{-12} to find the effective potentials for Lennard-Jones nanoparticles. Substituting $n = 12$ into the results of Sec. V A, and using the relations

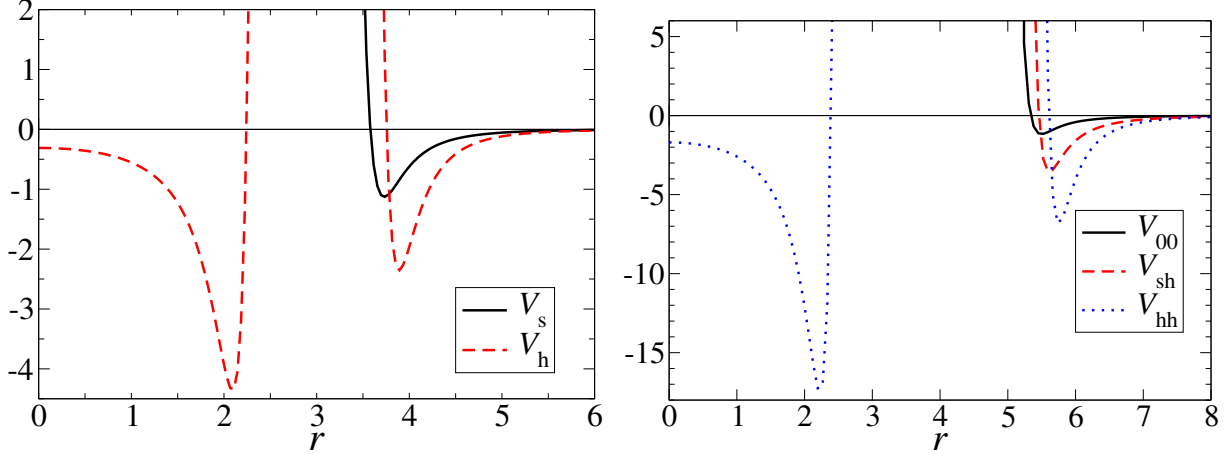


FIG. 7: Typical example of effective potentials based on the Buckingham potential for $a = e^{13}$, $b = 13$ and $c = 2$, with the cut-off r^* set to $1/4$. The left panel shows the effective potential for a point particle and a solid or hollow nanoparticle of radius $s = 3$, the right panel shows the potentials for two nanoparticles of radius $s_1 = 4$ and $s_2 = 1$.

between auxiliary and effective potentials, one finds

$$V_0^{12}(r) = \frac{4\pi s^3}{3(r^2 - s^2)^6} + \frac{80\pi s^9 + 432\pi r^4 s^5}{45(r^2 - s^2)^9} \quad (91)$$

$$V_h^{12}(r) = \frac{4\pi s^2}{(r^2 - s^2)^6} + \frac{64\pi r^2 s^4 (r^4 + \frac{6}{5}s^2 r^2 + s^4)}{(r^2 - s^2)^{10}} \quad (92)$$

$$V_{00}^{12}(r) = \frac{\pi^2}{37800r} \left[\frac{(r + \frac{7}{2}D)^2 + \frac{5}{4}D^2 - \frac{15}{2}d^2}{(r + D)^7} - \frac{(r + \frac{7}{2}d)^2 + \frac{5}{4}d^2 - \frac{15}{2}D^2}{(r + d)^7} \right. \\ \left. + \frac{(r - \frac{7}{2}D)^2 + \frac{5}{4}D^2 - \frac{15}{2}d^2}{(r - D)^7} - \frac{(r - \frac{7}{2}d)^2 + \frac{5}{4}d^2 - \frac{15}{2}D^2}{(r - d)^7} \right] \quad (93)$$

$$V_{sh}^{12}(r) = \frac{\pi^2 s_2}{1260r} \left[-\frac{r + \frac{9}{2}D + \frac{7}{2}d}{(r + D)^8} - \frac{r - \frac{9}{2}D - \frac{7}{2}d}{(r - D)^8} + \frac{r + \frac{9}{2}d + \frac{7}{2}D}{(r + d)^8} + \frac{r - \frac{9}{2}d - \frac{7}{2}D}{(r - d)^8} \right] \quad (94)$$

$$V_{hh}^{12}(r) = \frac{2\pi^2 s_1 s_2}{45r} \left[\frac{1}{(r + D)^9} + \frac{1}{(r - D)^9} - \frac{1}{(r + d)^9} - \frac{1}{(r - d)^9} \right]. \quad (95)$$

The potential V_{00}^{12} is in agreement with the result in the appendix of Ref. 1.

The point-nanoparticle potentials for the Lennard-Jones potential are now given by

$$V_0^{\text{LJ}}(r) = V_0^{12}(r) - 2V_0^6(r) \\ = \frac{4\pi s^3}{3(r^2 - s^2)^6} + \frac{80\pi s^9 + 432\pi r^4 s^5}{45(r^2 - s^2)^9} - \frac{8\pi s^3}{3(r^2 - s^2)^3} \quad (96)$$

$$V_h^{\text{LJ}}(r) = V_h^{12}(r) - 2V_h^6(r) \\ = \frac{4\pi s^2}{(r^2 - s^2)^6} + \frac{64\pi r^2 s^4 (r^4 + \frac{6}{5}s^2 r^2 + s^4)}{(r^2 - s^2)^{10}} - \frac{8\pi s^2}{(r^2 - s^2)^3} - \frac{16\pi s^4}{(r^2 - s^2)^4}. \quad (97)$$

Equation (96) is a more concise notation of the result of Roth and Balasubramanya [Eq. (2) in Ref. 14]. Likewise, the inter-nanoparticle interactions due to a Lennard-Jones potential

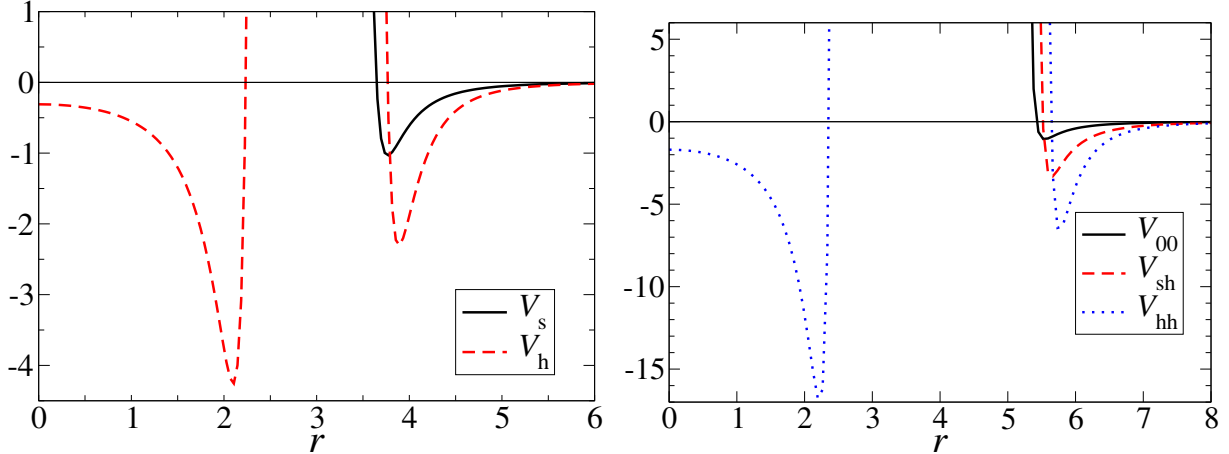


FIG. 8: Typical effective potentials based on the Lennard-Jones potential [Eqs. (96)–(98)]. On the left, the potential for a point particle and solid or hollow nanoparticle of radius $s = 3$ is shown, and on the right, the potentials for two nanoparticles of radius $s_1 = 4$ and $s_2 = 1$.

$i :$	0	1	2	3	4	5	6	7	8
α_i^{ss}	$-\frac{2^{13}}{315}$	$\frac{219136}{4725}$	$-\frac{24064}{675}$	$\frac{3456}{225}$	$-\frac{2^7}{45}$	$\frac{2^4}{9}$			
α_i^{sh}	$\frac{2^{15}}{315}$	$-\frac{2^{16}}{315}$	$\frac{2^{13}}{45}$	$-\frac{2^{12}}{45}$	$\frac{2^7}{3}$	$-\frac{2^8}{15}$	$\frac{2^4}{3}$		
α_i^{hh}	$\frac{2^{20}}{45}$	$-\frac{2^{18}}{5}$	$\frac{2^{18}}{5}$	$-\frac{917504}{30}$	$\frac{57344}{5}$	$-\frac{13312}{5}$	$\frac{14336}{15}$	2^7	2^4

TABLE I: Coefficients for the polynomials appearing in the effective inter-nanoparticle potentials based on the Lennard-Jones potentials, i.e., V_{00}^{LJ} , $V_{\text{sh}}^{\text{LJ}}$ and $V_{\text{hh}}^{\text{LJ}}$ in Eqs. (99)–(101).

are given by

$$V_{ij}^{\text{LJ}}(r) = V_{ij}^{12}(r) - 2V_{ij}^6(r), \quad (98)$$

where $ij = 00$, sh or hh . In Fig. 8, a typical example of these effective potentials is shown. Note the hard core part of the potentials. For the specific case of system of nanoparticles with the same radii $s_1 = s_2 = s$, studied in Ref. 23, the effective inter-nanoparticle interactions can be written in terms of $\eta = r/s$ as

$$V_{00}^{\text{LJ}}(r) = \frac{\pi^2 \sum_{i=0}^5 \alpha_i^{ss} \eta^{2i}}{s^6 \eta^8 (\eta^2 - 4)^7} - \frac{4\pi^2}{3} \frac{\eta^2 - 2}{\eta^2 (\eta^2 - 4)} - \frac{\pi^2}{3} \ln \left(1 - \frac{4}{\eta^2} \right) \quad (99)$$

$$V_{\text{sh}}^{\text{LJ}}(r) = \frac{\pi^2 \sum_{i=0}^6 \alpha_i^{sh} \eta^{2i}}{s^7 \eta^8 (\eta^2 - 4)^8} - \frac{32\pi^2}{3s \eta^2 (\eta^2 - 4)^2} \quad (100)$$

$$V_{\text{hh}}^{\text{LJ}}(r) = \frac{\pi^2 \sum_{i=0}^8 \alpha_i^{hh} \eta^{2i}}{s^8 \eta^{10} (\eta^2 - 4)^9} - 32\pi^2 \frac{\eta^4 + 6\eta^2 - 8}{s^2 \eta^4 (\eta^2 - 4)^3} \quad (101)$$

with the α coefficients given in Table I. Equation (101) is the so-called Girifalco potential.¹⁷

VI. ACCURACY OF THE LENNARD-JONES BASED EFFECTIVE POTENTIALS FOR FCC NANOPARTICLES

Since the effective potentials derived above are intended to model nanoparticles, it is natural to ask to what extent they can represent the interactions of nanoclusters composed

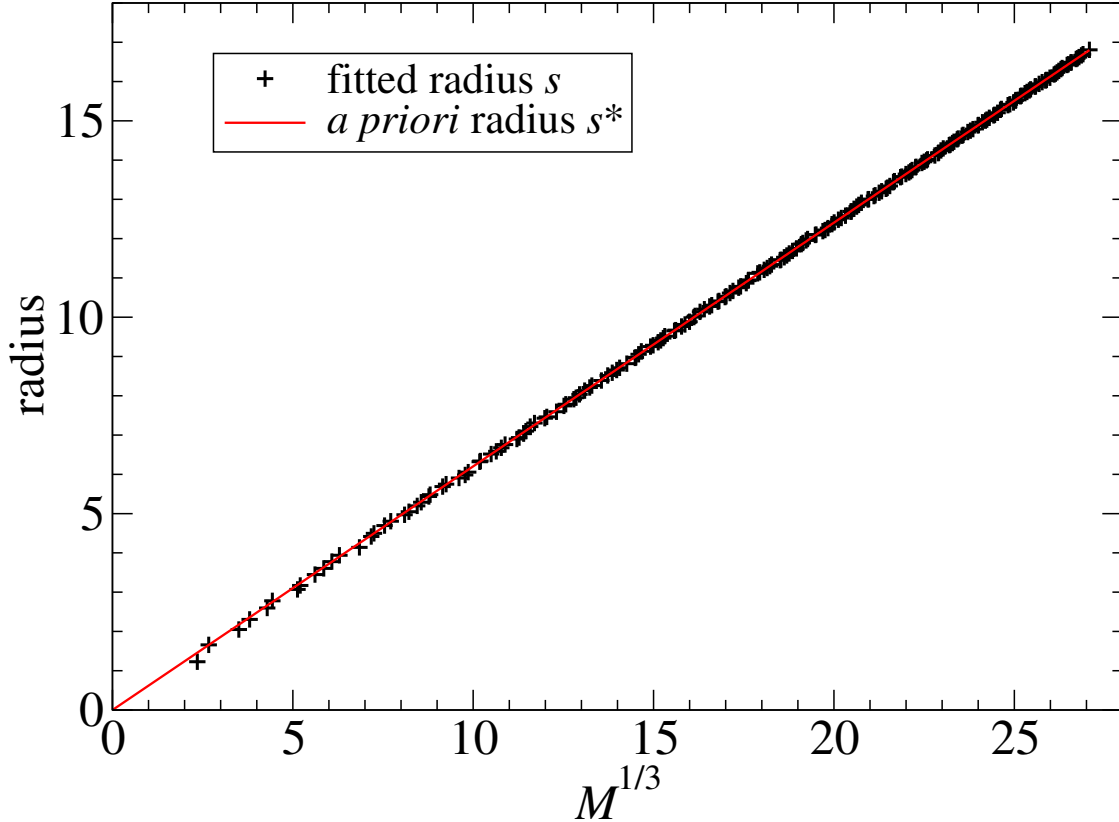


FIG. 9: Comparison of the fitted radius s and the *a priori* radius s^* of the fcc nanoparticles. The fit is based on minimizing $\Delta_{\text{pn}}(s)$, but minimizing $\Delta_{\text{nn}}(s)$ instead gives indistinguishable results.

of atoms. This obviously will depend on the structure of the nanoclusters, but to get at least a partial answer, the fcc-based nanoparticles of Sec. II will be used again, with the basic pair potentials ϕ_{pn} and ϕ_{nn} given by ϕ^{LJ} in Eq. (90). This potential has a minimum at $r = 1$, which sets the unit of length. The fcc nanoparticles are constructed from an fcc lattice with mean density $\bar{\rho} = 1$ by picking an atom and including all atoms within a given distance from it. Note that this gives only specific values for the number M of included atoms, since many atoms lie at the same distance in the crystal structure. Here, M will be restricted to less than 20,000, resulting in 206 clusters, the largest of which has $M = 19,861$ atoms.

The mean density $\bar{\rho} = 1$ for the fcc nanoparticles is not unrealistic: It results in a lattice distance $a = 4^{1/3}$ (Ref. 18, p. 12), i.e., the ratio of the lattice distance to the interaction range is $4^{1/3} \approx 1.587$. This is comparable to the case of platinum nanoparticles in water: Assuming the lattice distance a is the same as in a bulk platinum crystal, $a = 3.92 \text{ \AA}$ (Ref. 18, p. 23), and using that the interaction range of Pt atoms with water is of the order of 2 to 3 \AA ,²⁷ one finds a similar ratio of $3.92\text{\AA}/2.5\text{\AA} = 1.568$.

To test the applicability of describing these fcc nanoclusters as spheres with a constant density, one should compare the effective point-nanoparticle potential $V_{\text{pn}} = \rho V_0^{\text{LJ}}$ to the result of summing the potentials ϕ^{LJ} between the point particle and each of the atoms in the fcc nanoparticle. Similarly, the effective potential $V_{\text{nn}} = \rho^2 V_{00}^{\text{LJ}}$ between two equally sized nanoparticles should be compared to the result of summing the potentials between the each of the atoms of one of the nanoparticles with each of the atoms in the other.

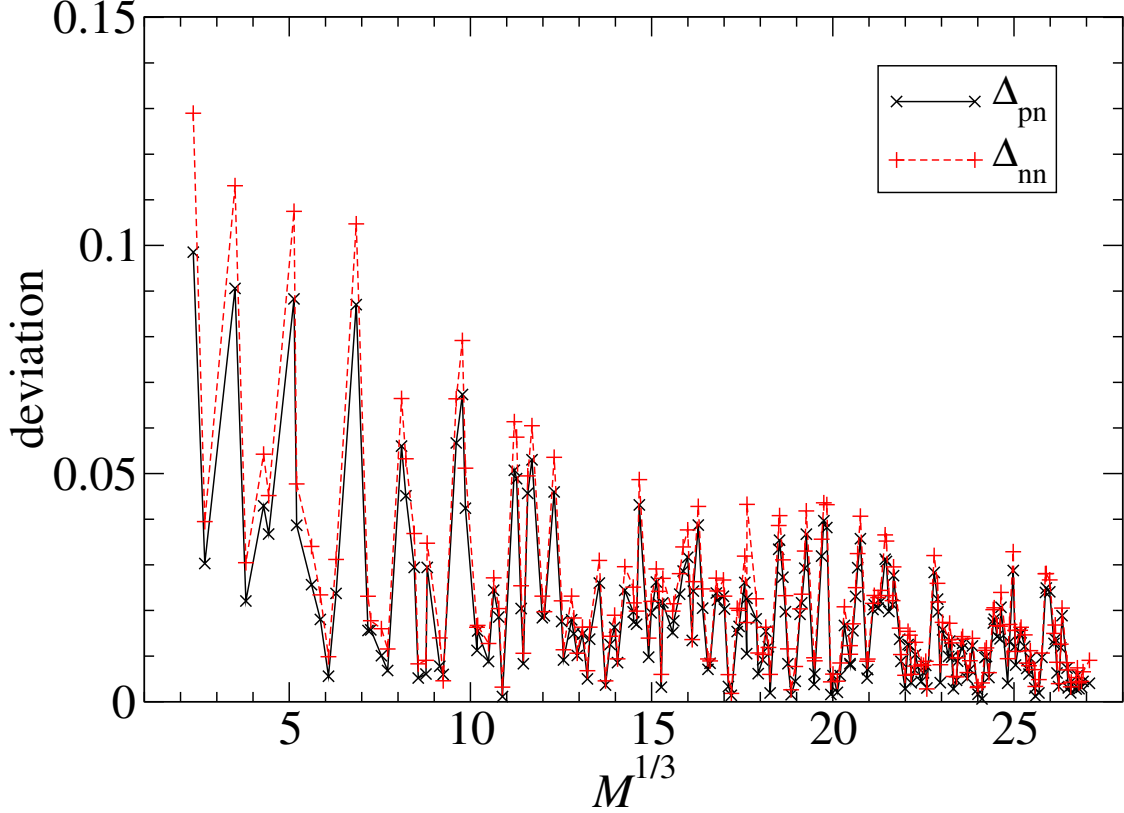


FIG. 10: Deviations Δ_{pn} and Δ_{nn} of the effective potentials from the atom-by-atom summed potentials for the fcc nanoparticles as a function of the fitted radius s .

However, there are two difficulties in performing these comparisons. First, the effective potentials are spherically symmetric, but the summed potentials will not be, since the fcc nanoparticles are not truly spherically symmetric. Therefore, the comparison will be made with the summed potentials averaged over all orientations of the nanoparticles, which will be denoted by $V_{\text{pn}}^{\text{sum}}$ and $V_{\text{nn}}^{\text{sum}}$.

The second problem with the comparison is that the radius s of the nanoparticle, which is a parameter in the effective potentials, is not well defined. A reasonable *a priori* radius would be $s^* = [3M/(4\pi\bar{\rho})]^{1/3}$, but other values for the radius s close to s^* are just as reasonable. Thus, the radius may be viewed as a fitting parameter, which will be adjusted to minimize the difference between the effective and the summed potential. To be precise, the following quantities are minimized by varying s :

$$\begin{aligned}\tilde{\Delta}_{\text{pn}} &= \left\{ \int' dr \left[V_{\text{pn}}^{\text{sum}}(r) - \rho(s)V_0^{\text{LJ}}(r) \right]^2 \right\}^{1/2} \\ \tilde{\Delta}_{\text{nn}} &= \left\{ \int' dr \left[V_{\text{nn}}^{\text{sum}}(r) - \rho^2(s)V_{00}^{\text{LJ}}(r) \right]^2 \right\}^{1/2}\end{aligned}\quad (102)$$

Here, $\rho(s) = 3M/(4\pi s^3)$, and the prime denotes the restriction on the integration that $V_{\text{pn}}^{\text{sum}}(r) < 3V_{\text{pn}}^*$ or $V_{\text{nn}}^{\text{sum}}(r) < 3V_{\text{nn}}^*$, respectively, where V_{pn}^* and V_{nn}^* are the absolute value of the minima of $V_{\text{pn}}^{\text{sum}}$ and $V_{\text{nn}}^{\text{sum}}$. The restriction is needed to make the integrals converge. The results depend very little on the precise choice of the restriction. For instance, changing the restriction to $2V^*$ instead of $3V^*$, shifts the values for the radii s only by an amount of

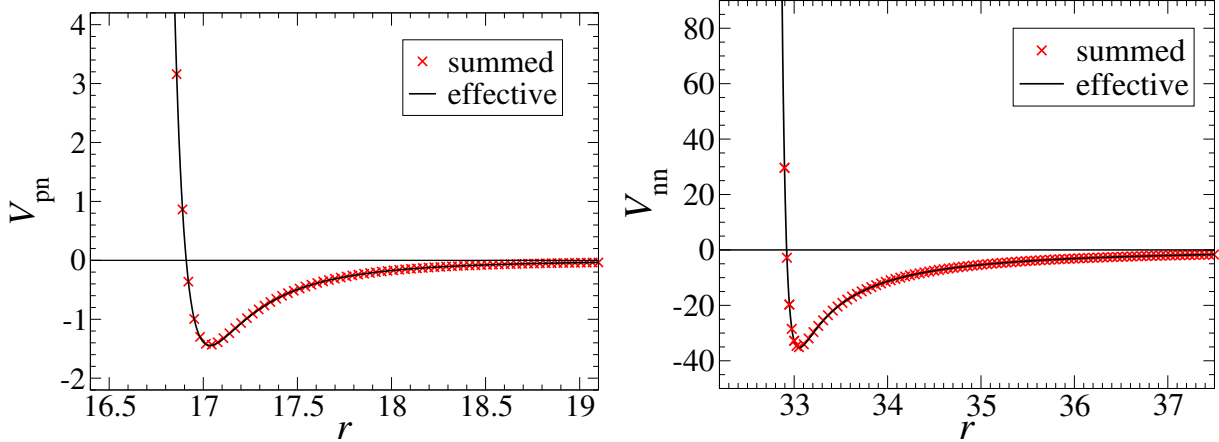


FIG. 11: An example of very good agreement between the effective and summed potentials, which occurs for an fcc nanocluster of size $M = 18053$ with an effective radius of 16.27 (in dimensionless units). Crosses represent the orientationally averaged summed potentials $V_{\text{pn}}^{\text{sum}}$ (left) and $V_{\text{nn}}^{\text{sum}}$ (right), while the solid lines are the effective potentials $V_{\text{pn}} = \rho V_0^{\text{LJ}}$ (left) and $V_{\text{nn}} = \rho^2 V_{00}^{\text{LJ}}$ (right).

the order of 10^{-4} .

The values of the radius that result from minimizing Δ_{pn} for the 206 cluster configurations with $M < 20,000$ are shown in Fig. 9. It is seen that with the exception of some of the smaller clusters, the values of fitted radii s typically lie close very to the *a priori* radius s^* . Minimizing Δ_{nn} instead results in the same values for the radii to within 0.3%.

To get an idea of the accuracy of the fit as a function of the size of the nanoparticles, one may investigate the values of the dimensionless deviations

$$\Delta_{\text{pn}} = \frac{\tilde{\Delta}_{\text{pn}}}{R_{\text{pn}}^{1/2} V_{\text{pn}}^*}; \quad \Delta_{\text{nn}} = \frac{\tilde{\Delta}_{\text{nn}}}{R_{\text{nn}}^{1/2} V_{\text{nn}}^*}.$$

The length scales R_{pn} and R_{nn} are chosen as the lengths of the intervals contributing 99.9% of the values of the integrals in Eqs. (102). This typically gives $R_{\text{pn}} \approx 1.35$ and $R_{\text{nn}} \approx 2$ for the size of clusters investigated here, and these values of R_{pn} and R_{nn} were used for all clusters. The dimensionless deviations are plotted in Fig. 10. One sees a high degree of correlation between the accuracy of the effective potential for a nanoparticle and point particle and the accuracy of the effective inter-nanoparticle potential. The deviations are furthermore typically small, indicating that there is good agreement between the effective potentials and the sum of atom-atom potentials, although the deviations are larger for specific cluster sizes. As extreme examples, Fig. 11 shows a case of very good agreement and Fig. 12 shows a case of poor agreement. In these figures, the effective potentials and the summed potentials are compared for $M = 18053$ with $s = 16.27$ and $M = 17357$ with $s = 16.04$, respectively. Note that the agreement is never very bad, but for the latter, the depth of the minimum is somewhat underestimated by the effective potentials, as the insets of Fig. 12 show.

It is hard to say in general why the smooth, constant density description works better for some clusters than for others. For some of the smaller nanoclusters with poorer agreement, inspecting the spatial structure of the nanocluster shows a rather rough surface, which could be the explanation. But for the larger nanoparticles, such a difference in roughness is hard to distinguish.

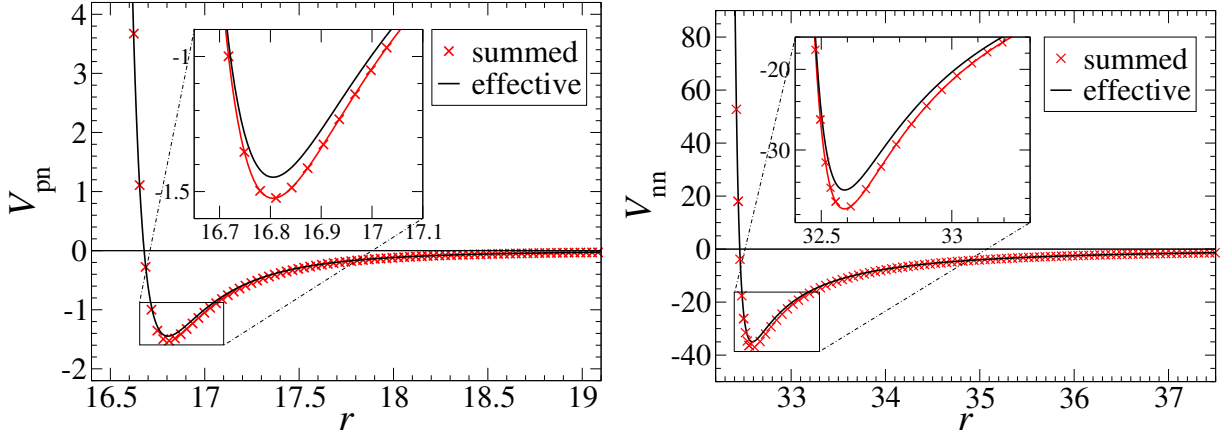


FIG. 12: An example of poorer agreement between the effective and summed potentials, which occurs for an fcc nanocluster of size $M = 17357$ with an effective radius of 16.04 (dimensionless units). Solid lines represent the effective potentials $V_{pn} = \rho V_0^{LJ}$ (left) and $V_{nn} = \rho^2 V_{00}^{LJ}$ (right), while crosses are the orientationally averaged summed potentials V_{pn}^{sum} (left) and V_{nn}^{sum} (right) which result from the sum over the atoms. The inset in the right plot zooms in on the minimum, and shows that its depth is underestimated by the effective potential.

VII. DISCUSSION

A general effective description for nanoparticles was presented, starting from a smoothing procedure in which the real spatial density profile inside the nanoparticles is replaced by a spherically symmetric one. The resulting effective interactions between a nanoparticle and a point particle as well as between two nanoparticles are then given by spherically symmetric potentials, thus greatly simplifying the description over an all-atom model.

The main results of this approach are the formulation of the effective potentials in terms of auxiliary potentials, Eqs. (17) and (18), which provide a unified description of overlapping and non-overlapping configurations. The auxiliary potentials are related to the basic interaction potentials through Eqs. (19) and (20). Furthermore, the effective potentials for hollow particles were found to be related to those for solid nanoparticles by simple differentiation with respect to the radii of the nanoparticles, see Eqs. (47) and (50), and as such also allow a formulation in terms of auxiliary potentials, as given in Sec. IV.

As an application of the formalism, explicit effective pair potentials for solid and hollow nanoparticles were obtained for various basic pair potentials. Different pair potentials have different applications. For instance, the Lennard-Jones potential is a general-purpose potential, while the Buckingham potential is suited to describe the physics of particles close together such as in high pressure systems. These basic potentials result in effective nanoparticle potentials with hard cores plus a soft potential. They reduce in limiting cases to some of the existing model potentials for colloids, such as hard spheres and the Hamaker potential,^{10,16,19} but not to more ad hoc models such as the description of a colloid as a single big Lennard-Jones particle.²⁰ In contrast, the Morse potential is able to describe bounded systems or penetrable particles, making it possible to model nanoparticles that could passively capture and trap specific types of particles. This could have applications in modeling drug delivery by nanoparticles⁸ and viral capsids.⁹

For the case of a Lennard-Jones basic potential, a comparison was carried out with

an atomic model of a nanocluster. In this model, the atoms making up the nanoparticle were assumed to be arranged in an fcc lattice structure. To find approximate spherical structures, the atoms were restricted to lie within a certain distance from the central atom in the nanocluster. Configurations with up to 19,861 atoms were studied. The effective potentials were compared with the orientationally averaged sum of Lennard-Jones potentials due to the individual atoms. The agreement tends to be very good, provided the radius in the effective description is treated as a fitting parameter. For some configurations, however, the fitting procedure underestimates the depth of the minimum of the potentials. This may be due to surface roughness of these structures, which is caused by the imposed fcc structure and unlikely to be relevant for real nanoclusters.

The application of the explicit expressions for the effective potentials to numerical studies of spherical nanoparticles is in principle straightforward. In fact, the potentials in Eqs. (96) and (99) have already been used in a numerical study of single particle transport in an equilibrium nanofluid composed of solid nanoparticles and fluid particles interaction through Lennard-Jones interactions, where the validity of a Gaussian approximation of the Van Hove self-correlation function was investigated, and found to hold up to picosecond time scales for the fluid particles, and up to five to ten times longer (depending on temperature) for nanoparticles with a size of about 2 nm.²³

Given the explicit expressions for the effective potentials, the description allows a fairly direct route toward a qualitative model for a given system of nanoparticles in a fluid, since reasonable values for the parameters for commonly used pair potentials are available in the literature,²⁸ while the number of atoms in a nanoparticle and its radius could be taken from experiments or theoretical calculations.¹¹ Furthermore, the effective potentials have a physical range based on the interaction of their constituents rather than on their radius. Therefore, the effective potentials that were derived here are expected to be useful for the qualitative description of a wide variety of systems, from mono-disperse nanoparticles in a fluid to mixtures of different kinds of fluid particles, nanoclusters or buckyballs.

A number of interesting extensions present themselves for future research. For instance, while the nanoparticles were assumed to be composed of one kind of particle only, potentials for nanoparticles composed of several types of particles can also be derived within the current context if the distribution of the types is either homogeneously mixed or distributed in spherical shells (so-called core-shell nanoparticles^{6,29}). The spherical symmetry of the effective potentials, which decouples the rotational and translational degrees of freedom, could be lifted to extend the model to include rotational motion. This may be done by adding interaction sites on the surface of the nanoparticle or a multipole expansion. As long as the orientationally dependent potential is available, there are no obstacles in molecular dynamics simulations of such systems.³⁰ Furthermore, combining the current model with the mesoscopic fluid model of Malevanets and Kapral³¹ would yield a numerically efficient model of larger nanoparticles and colloids that includes hydrodynamic effects. These avenues are currently being investigated.

Acknowledgments

The author wishes to thank Profs. E. G. D. Cohen, R. Kapral, and J. Schofield for useful discussions. This work was supported by the National Sciences and Engineering Research Council of Canada and a Petroleum Research Fund from the American Chemical Society.

APPENDIX A: THE KERNEL K_{ij}

The integral in the expression for the kernel K_{ij} in Eq. (14) will be worked out now. Using Eq. (9) and the binomial formula for $(x - y)^{i+2}$, one finds, after resummation, that

$$\begin{aligned} K_{ij}(x, s_1, s_2) &= \int_{y_1}^{y_2} dy \frac{4\pi^2 \Theta(D - |x|)}{(i+2)(j+2)} [s_1^{i+2} - (x-y)^{i+2}] [s_2^{j+2} - y^{j+2}] \quad (\text{A1}) \\ &= \frac{4\pi^2 \Theta(D - |x|) s_1^{i+2} s_2^{j+2}}{(i+2)(j+2)} \left[y - \frac{s_1}{i+3} \left(\frac{x+y}{s_1} \right)^{i+3} \right. \\ &\quad \left. + \frac{s_2}{j+3} \left(\frac{y}{s_2} \right)^{j+3} \left\{ \left(\frac{x}{s_1} \right)^{i+2} F \left(-i-2, j+3; j+4; -\frac{y}{x} \right) - 1 \right\} \right]_{y_1}^{y_2}, \quad (\text{A2}) \end{aligned}$$

where $y_1 = \max(-s_2, x - s_1)$ and $y_2 = \min(s_2, x + s_1)$, which are due to the finite support of the kernels K_i and K_j , and F is the hypergeometric function.³² Despite its complicated appearance, Eq. (A2) is simply a piecewise polynomial in x of degree $i + j + 5$ at most. To see this, it is useful to distinguish the following four non-trivial cases: *case 1*: $x > 0$ and $|d| < |x| < D$, for which $y_1 = x - s_1$ and $y_2 = s_2$; *case 2*: $d > 0$ and $|x| < |d|$, giving $y_1 = -s_2$ and $y_2 = s_2$; *case 3*: $d < 0$ and $|x| < |d|$, giving $y_1 = x - s_1$ and $y_2 = x + s_1$; and *case 4*: $x < 0$ and $|d| < |x| < D$, for which $y_1 = -s_2$ and $y_2 = x + s_1$. There are in fact only two independent cases, because case 3 can be obtained from the result of case 2 by interchanging s_1 and s_2 as well as i and j (which will also flip the sign of d), while the result for case 4 can be obtained from that of case 1 by setting s_1 to $-s_2$, s_2 to $-s_1$ and introducing a minus sign, as can be proved by changing the integration variable in Eq. (A1) from y to $x - y$. Thus, one only needs to consider the cases 1 and 2. Changing the integration variable from y to $z = s_2 - y$ and using the binomial formula, Eq. (A1) for case 1 yields

$$K_{ij}(x, s_1, s_2) = (i+2)!(j+2)! \sum_{m=0}^{i+j+2} \frac{(D-x)^{m+3}}{(m+3)!} \sum_{k=\max(1, m-j)}^{\min(i+2, m+1)} \frac{(-s_1)^{i+2-k}}{(i+2-k)!} \frac{s_2^{j-m+k}}{(j-m+k)!} \quad (\text{A3})$$

which is polynomial in x of degree $i + j + 5$, while for case 2 the integral in Eq. (A1) can be found by using the binomial formula for $(x - y)^{i+2}$, giving a polynomial of degree $i + 2$, i.e.

$$K_{ij}(x, s_1, s_2) = \frac{8\pi^2 s_2^{j+3}}{i+2} \left[\frac{s_1^{i+2}}{j+3} - \sum_{k=0}^{i/2+1} \binom{i+2}{2k} \frac{s_2^{i+2-2k} x^{2k}}{(i+3-2k)(i+j+5-2k)} \right]. \quad (\text{A4})$$

¹ U. S. Schwarz and S. A. Safran, Phys. Rev. E **62**, 6957 (2000).

² S. U. S. Choi *et al.*, in *DOE BES 20th Symposium on Energy Engineering Sciences*. Argonne, IL May 20-21, 2002.

³ H. J. Hwang, O.-K. Kwon and J. W. Kang, Solid State Comm. **129**, 687 (2004); W. Tang and S. G. Advani, J. Chem. Phys. **125**, 174706 (2006).

⁴ X. Chen *et al.*, J. Am. Chem. Soc. **127**, 4372 (2005).

⁵ R. Verberg, I. M. de Schepper and E. G. D. Cohen, Phys. Rev. E **55**, 3143 (1997).

⁶ S. C. Glotzer, M. J. Solomon and N. A. Kotov, AIChE J. **50**, 2978 (2004).

- ⁷ P. R. ten Wolde and D. Frenkel, *Science* **277**, 1975 (1997); G. Pellicane, D. Costa and C. Caccamo, *J. Phys.: Condens. Matter* **16**, S4923 (2004).
- ⁸ R. Jurgons *et al.*, *J. Phys.: Condens. Matter* **18** S2893 (2006); M. Arruebo *et al.*, *Chem. Mater.*, **18**, 1911 (2006).
- ⁹ R. L. Garcea and L. Gissmann, *Curr. Opin. Biotechnol.* **15**, 513 (2004).
- ¹⁰ J. L. Barrat and J. P. Hansen, *Basic concepts for simple and complex liquids* (Cambridge University Press, Cambridge, 2003).
- ¹¹ F. Baletto and R. Ferrando, *Rev. Mod. Phys.* **77**, 371 (2005).
- ¹² N. Gonzalez Szwacki, A. Sadrzadeh and B. I. Yakobson, *Phys. Rev. Lett.* **98**, 166804 (2007); G. Gopakumar, M. T. Nguyen and A. Ceulemans, *Chem. Phys. Lett.* **450**, 175 (2008).
- ¹³ S. Bhattacharjee and M. Elimelech, *J. Colloid Interface Sci.* **193**, 273 (1997).
- ¹⁴ M. W. Roth and M. K. Balasubramanya, *Phys. Rev. B* **62**, 17043 (2000).
- ¹⁵ M. K. Balasubramanya and M. W. Roth, *Phys. Rev. B* **63**, 205425 (2001).
- ¹⁶ H. C. Hamaker, *Physica* **4**, 1058 (1937).
- ¹⁷ L. A. Girifalco, *J. Phys. Chem.* **96**, 858 (1992).
- ¹⁸ C. Kittel, *Introduction to Solid State Physics*, (John Wiley and Sons, New York, 1986) 6th ed.
- ¹⁹ B. V. Derjaguin and L. V. Landau, *Acta Phys. Chim. USSR* **14**, 633 (1941); E. J. W. Verwey and J. T. G. Overbeek, *Theory of Stability of Lyophobic Colloids* (Elsevier, Amsterdam, 1948); B. Cichocki and B. U. Felderhof, *J. Chem. Phys.* **89**, 1049 (1988); B. Cichocki and K. Hinszen, *Physica A* **166**, 473 (1990).
- ²⁰ S. H. Lee and R. Kapral, *J. Chem. Phys.* **121**, 11163 (2004).
- ²¹ This notation is similar to the so-called Bach brackets used to denote symmetrized and anti-symmetrized tensors in general relativity, see e.g. H. Stephani, *General Relativity: an Introduction to the Theory of the Gravitational Field*, 2nd ed. (Cambridge University Press, 1990).
- ²² J. E. Lennard-Jones, *Physica* **4**, 941 (1937).
- ²³ R. van Zon, S. S. Ashwin and E. G. D. Cohen, *Nonlinearity* **21**, R119 (2008).
- ²⁴ P. M. Morse, *Phys. Rev.* **34**, 57 (1929).
- ²⁵ L. A. Girifalco and V. G. Weizer, *Phys. Rev.* **114**, 686 (1959).
- ²⁶ R. A. Buckingham, *Proc. Roy. Soc.* **168A**, 264 (1938).
- ²⁷ See e.g. E. Spohr, *J. Phys. Chem.* **93**, 6171 (1989).
- ²⁸ A. D. MacKerell *et al.*, *J. Phys. Chem. B* **102**, 3586 (1998).
- ²⁹ V. Molinero, D. Laria and R. Kapral, *Phys. Rev. Lett.* **84**, 455 (2000).
- ³⁰ R. van Zon and J. Schofield, *Phys. Rev. E* **75**, 056701 (2007); R. van Zon, I. Omelyan and J. Schofield, *J. Chem. Phys.* **128**, 136102 (2008).
- ³¹ A. Malevanets and R. Kapral, *J. Chem. Phys.* **110**, 8605 (1999); *ibid.* **112**, 7260 (2000).
- ³² I. S. Gradshteyn and I. M. Ryzhik, *Table of Integrals, Series, and Products* (Academic Press, San Diego, 2000).